

# Quantum Many-Body Scars in Optical Lattices

Hongzheng Zhao,<sup>1,\*</sup> Joseph Vovrosh,<sup>1</sup> Florian Mintert,<sup>1</sup> and Johannes Knolle<sup>2,3,1</sup>

<sup>1</sup>*Blackett Laboratory, Imperial College London, London SW7 2AZ, United Kingdom*

<sup>2</sup>*Department of Physics TQM, Technische Universität München,  
James-Frank-Straße 1, D-85748 Garching, Germany*

<sup>3</sup>*Munich Center for Quantum Science and Technology (MCQST), 80799 Munich, Germany*  
(Dated: April 27, 2020)

The concept of quantum *many-body scars* has recently been put forward as a route to describe weak ergodicity breaking and violation of the Eigenstate Thermalization Hypothesis. We propose a simple setup to generate quantum many-body scars in a doubly modulated Bose-Hubbard system which can be readily implemented in cold atomic gases. The dynamics are shown to be governed by kinetic constraints which appear via density assisted tunneling in a high-frequency expansion. We find the optimal driving parameters for the kinetically constrained hopping which leads to small isolated subspaces of scarred eigenstates. The experimental signatures and the transition to fully thermalizing behavior as a function of driving frequency are analyzed.

*Introduction.*— There have been great efforts in the last decades to further our understanding of quantum thermalization, *i.e.* how local observables of a closed quantum system converge to a stationary state of thermal equilibrium, even though the system follows unitary dynamics. It is believed, with strong support from extensive numerical studies [1], that quantum thermalization can be sufficiently described by the Eigenstate Thermalization Hypothesis (ETH) [2]. Additional evidence comes from the rapid progress in controllable experiments, for example cold atoms [3–5] and trapped ions [6, 7], which have enabled the characterization of different paths to thermalization [8].

While ETH can explain thermalization for the vast majority of quantum systems, there are also systems substantially deviating from predictions by ETH, as observed in quench experiments showing that some systems keep some memory of their initial state [9]. Prominent examples include integrable systems [10] and many-body localized (MBL) phases [11–13] with an extensive number of conserved quantities. Beyond the two extremes of fully thermalizing versus fully many-body localized systems, the basic question has emerged whether ergodicity can be weakly broken by special eigenstates rather than the full spectrum.

Recently, an interesting phenomenon suggesting weak ergodicity breaking in non-integrable systems was observed experimentally on a Rydberg atom platform [5]. Unexpected persistent coherent oscillations appeared for a set of special initial states. It turns out that kinetic constraints in the system play an important role in the appearance of slow equilibration; for example the constrained PXP model of a spin- $\frac{1}{2}$  chain [14–19] displays similar phenomenology. A special band of non-thermal eigenstates, dubbed *quantum many-body scars*, emerge; they have support in a small portion of Fock-space while other states obey ETH. Any initial state with a large overlap with scar states displays non-ergodic behavior that manifests itself through persistent coherent oscilla-

tions.

By now, there exist several theoretical proposals for quantum systems hosting quantum many-body scars; most of them are spin models [14, 15, 20–31], but also fermionic [32, 33] and bosonic models [34] can show this effect. Besides the spin-model realized with Rydberg atoms, all of these models are designed such that they feature quantum many-body scars with little consideration on actual implementability. A crucial question is whether quantum many-body scars can also occur in experimentally feasible settings beyond spin systems.

We propose an experiment consisting of bosonic atoms trapped in an optical lattice, with temporal modulation of on-site energy and interaction. In the fast driving regime, this can be described by an effective model [35, 36] with density-assisted tunneling processes, such that the rate for a particle to tunnel depends on the number of particles on its site and neighboring sites. Since these rates can be tuned in terms of driving amplitudes and frequencies, optimally chosen driving parameters realize *kinetic constraints*, *i.e.* selection rules between states that would otherwise be connected via tunneling processes. For the effective model, the Hilbert space is then separated into disjoint subspaces, leading to the appearance of quantum many-body scars [33]. We show that scarred states are experimentally detectable from suitable initial states that result in coherent oscillations that exist for time-scales exceeding the natural time-scales for thermalization by far.

*Doubly Modulated Model.*— We focus on a system of spinless bosons occupying the lowest band in an 1D optical lattice described by the Bose Hubbard Model (BHM),

$$\hat{H}(t) = \sum_{\langle pq \rangle} \hat{c}_p^\dagger J_{pq} \hat{c}_q + \frac{U(t)}{2} \sum_p \hat{n}_p (\hat{n}_p - 1) + F(t) \sum_p \epsilon_p \hat{n}_p, \quad (1)$$

where  $\hat{c}_p$  ( $\hat{c}_p^\dagger$ ) annihilates (creates) a boson at site  $p$ , and  $\hat{n}_p = \hat{c}_p^\dagger \hat{c}_p$  is the occupation number operator.  $U(t)$  is the amplitude of the on-site interaction,  $\epsilon_p = -p$  repre-

sents the tilt potential,  $F(t)$  is the shaking amplitude, and  $J_{pq} = -J$  is the bare tunneling rate between nearest neighbors. We will consider the doubly modulated version of the BHM [37, 38], in which both  $U(t)$  and  $F(t)$  are modulated periodically with period  $T$ . In practice, the time dependence results from a periodic tilt or acceleration of the lattice and modulation of a magnetic field inducing a Feshbach resonance [39, 40]. We exploit the freedom to choose suitable driving profiles to realize kinetically constrained hopping of bosons on a chain. It turns out that a monochromatically modulated on-site interaction  $U(t) = U_d \cos(\omega t)$  and a shaking in the form  $F(t) = F_2 \cos(2\omega t) + F_4 \cos(4\omega t)$  are all that is required. To simplify notation, we will also use the dimensionless quantities  $\tilde{U}_d = U_d/\omega$ ,  $\tilde{F}_2 = F_2/2\omega$  and  $\tilde{F}_4 = F_4/4\omega$  in the following.

*Kinetically Constrained Hopping.*– The Hamiltonian  $\tilde{H}(t)$  in the frame induced by the driving term of the Hamiltonian admits a perturbative high-frequency expansion even for strong driving [37, 38]. The dynamics can then be approximated by a time-independent effective Hamiltonian  $\hat{H}_{\text{eff}}$  [41]. The lowest order contribution to the high-frequency expansion reads  $\hat{H}_{\text{eff}}^0 = \frac{1}{T} \int_0^T dt \tilde{H}(t)$ , which in the present case reduces to the so-called density assisted tunneling

$$\hat{H}_{\text{eff}}^0 = \sum_{pq} \hat{c}_p^\dagger \hat{A}_{pq}^0(\hat{n}_p, \hat{n}_q) \hat{c}_q, \quad (2)$$

where the density dependence is contained in the operator

$$\hat{A}_{pq}^0(\hat{n}_p, \hat{n}_q) = -J \mathcal{J}_0(\tilde{U}_d(\hat{n}_p - \hat{n}_q), \tilde{F}_2(p - q), \tilde{F}_4(p - q)), \quad (3)$$

in terms of the zeroth order three-dimensional Bessel function  $\mathcal{J}_0$  [42]. The existence of the term  $\hat{n}_p - \hat{n}_q$  in the operator  $\hat{A}_{pq}^0$  indicates that the tunneling rates depend on the occupation number difference of specific initial and final states [37, 38]. For example, in a chain with the initial Fock state  $|\psi_i\rangle = |n_1 \dots n_N\rangle$  one obtains

$$\hat{c}_p^\dagger \hat{A}_{p,p+1}^0 \hat{c}_{p+1} |\psi_i\rangle = h_{n_p, n_{p+1}}^L \hat{c}_p^\dagger \hat{c}_{p+1} |\psi_i\rangle, \quad (4)$$

with the prefactor

$$h_{n_p, n_{p+1}}^L = -J \mathcal{J}_0(\tilde{U}_d(-n_p + n_{p+1} - 1), \tilde{F}_2, \tilde{F}_4), \quad (5)$$

that can be interpreted as the tunneling rate for a particle to tunnel from site  $p + 1$  to  $p$ , *i.e.* to the left. Similarly the rate for a particle to tunnel from site  $p$  to  $p + 1$  reads

$$h_{n_p, n_{p+1}}^R = -J \mathcal{J}_0(\tilde{U}_d(-n_p + n_{p+1} + 1), \tilde{F}_2, \tilde{F}_4). \quad (6)$$

As states with low occupations per site will be particularly relevant, the following rates

$$\begin{aligned} h_{(0,1)}^L &= h_{(1,0)}^R = h_{(2,1)}^R = h_{(1,2)}^L = -J \mathcal{J}_0(0, \tilde{F}_2, \tilde{F}_4), \\ h_{(1,1)}^{L/R} &= h_{(2,0)}^R = h_{(0,2)}^L = -J \mathcal{J}_0(\tilde{U}_d, \tilde{F}_2, \tilde{F}_4), \\ h_{(2,1)}^L &= h_{(1,2)}^R = h_{(0,3)}^L = h_{(3,0)}^R = -J \mathcal{J}_0(2\tilde{U}_d, \tilde{F}_2, \tilde{F}_4), \end{aligned} \quad (7)$$

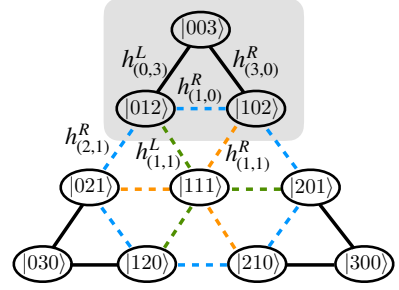


FIG. 1: Fragments for a system of 3 sites. Connections are assigned with hopping rates. If all dashed ones are forbidden for conditions in Eq. (8), four blocks of states appear. For clarity one of these is shadowed in gray.

play an important role in the formation of many-body scars.

*Fragmentation in Fock-Space.*– In order to understand how specific choices of the rates in Eq. (7) result in the desired fragmentation of Hilbert space, it is instructive to consider the basic example of three lattice sites with periodic boundary condition as illustrated in Fig. 1. Tunneling processes between different Fock states are indicated by solid and dashed lines, and processes that occur with the same rate are depicted with the same color.

If all the rates of processes depicted with dashed lines vanish, then the Hilbert space is being fragmented into four blocks – one block containing the states  $|012\rangle$ ,  $|102\rangle$ ,  $|003\rangle$ , two blocks containing their cyclic permutations, and the one-dimensional block  $|111\rangle$ . This fragmentation naturally occurs if the rates specified in Eq. (7) satisfy the conditions

$$h_{(2,0)}^R = h_{(0,2)}^L = h_{(1,1)}^{L/R} = 0, \quad h_{(1,2)}^L = h_{(2,1)}^R = 0. \quad (8)$$

In practice it is not necessary that these rates vanish exactly, but clear deviation from ETH can also be observed in the presence of *leaking channels*, *i.e.* small, but finite amplitudes of these rates.

Fragmentation in systems of any number of sites and filling factor can be understood in terms of elementary building blocks of few sites. One exemplary building block contains only the Fock states  $|n_1 n_2 n_3 n_4 n_5 n_6\rangle$  for a system of six atoms on six sites, with  $n_1 = n_6 = 0$ ,  $n_2 \leq 2$  and  $n_5 \leq 2$ , for instance the state  $|\psi\rangle = |003300\rangle$ . Due to the constraints in Eq. (8), the vanishing occupation on sites 1 and 6 in  $|\psi\rangle$  is conserved throughout time evolution. In turn, for a products of such 6-site states, there will be no mixing in-between thus they form a fragment which is much smaller than the total Hilbert space. In practice, there are many more elementary building blocks, giving rise to a substantial number of scarred states in large systems.

*Optimal Control of Scars.*– In order to realize the above scars experimentally, the driving parameters need to be

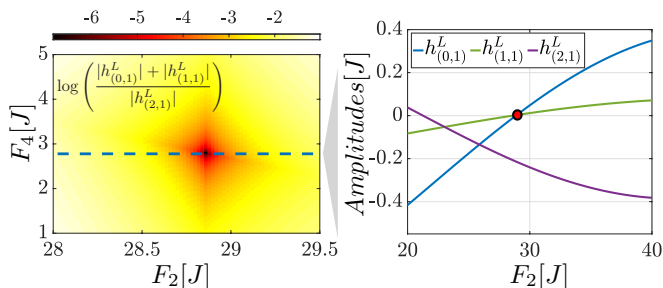


FIG. 2: Left: Figure of merit for the appearance of quantum many-body scars given by the ratio (log scale) of leaking and hopping channels for a Hilbert space fragment. The red region labels the best parameter space with ratios lower than  $10^{-4}$ . Right: Hopping rate as a function of  $F_2$ . Two leaking channels cross zero at the same time.

chosen such that

$$\mathcal{J}_0(\tilde{U}_d, \tilde{F}_2, \tilde{F}_4) = 0, \quad \mathcal{J}_0(0, \tilde{F}_2, \tilde{F}_4) = 0, \quad (9)$$

to satisfy the conditions given in Eq. (8). In general, one needs a large modulating interaction  $U_d$ , to realize a notable difference between hopping channels (Eq. (7)) with different particle numbers. For concreteness, we fix  $U_d/J = 12, \omega/J = 6$  and show the ratio between dominant leaking and leading hopping rates within the fragment ( $|h_{(0,1)}^L| + |h_{(1,1)}^L|$ ) /  $|h_{(2,1)}^L|$  as a function of  $F_2, F_4$  in the left panel of Fig. 2. This is a suitable figure of merit for the appearance of long time coherent oscillations as the inverse of the ratio captures the time scale for the leaking effects to become notable. There is a sweet spot in black around (28.8, 2.8) with ratios below  $10^{-6}$ . In the right panel, the rates are depicted with fixed  $F_4 = 2.8J$ , and one can see two leaking rates crossing zero at the same point. Therefore those two channels can be tuned to both be strictly forbidden, leading to perfect fragments.

So far we have restricted our discussion on the conditions for fragmentation of the Hilbert space of the effective Hamiltonian  $\hat{H}_{\text{eff}}^0$ , which drastically changes the stroboscopic dynamics of the driven Bose-Hubbard chain in the high-frequency regime, but higher order processes of magnitude  $O(1/\omega)$  will play an increasing role for smaller frequencies. This will inevitably open leaking channels and a transition to a thermalizing system without scars is expected. In the following, higher order effects are analyzed via the spectrum of the full Floquet operator,  $\hat{U}(T) = \mathcal{T} \int_0^T \exp(-i\hat{H}(t)dt)$ , obtained via exact diagonalization for unit-filling. The ratio between the driving amplitude  $U_d, F_2, F_4$  and frequency  $\omega$  is fixed to the optimal point discussed above.

In contrast to the smooth dependence of expectation values of local observables as a function of eigenstates' energy, scarred states typically lead to very different values even for states close in energy [27]. This violation

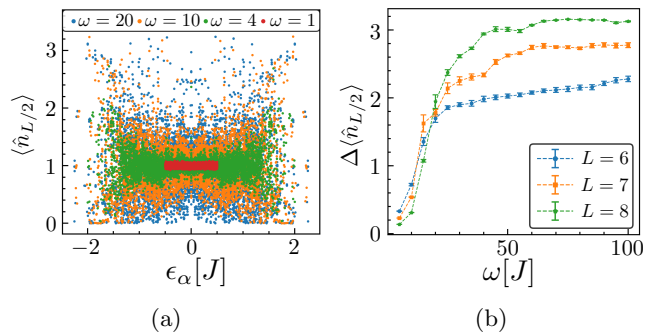


FIG. 3: Violation of ETH as a function of driving frequency in units of  $J$ . (a) Expectation value of the local particle number operator, with respect to eigenstates of the Floquet operator as function of the quasienergy for system size  $L = 8$ . (b) Width of the distribution of  $\langle \hat{n}_{L/2} \rangle$  as a function of frequency for different system sizes.

of ETH can be seen in Fig. 3a depicting the expectation value of the local particle number  $\langle \hat{n}_{L/2} \rangle$  for eigenstates of the Floquet operator as a function of their quasienergy. In the case of slow driving, depicted in red, the local particle number is close to the value of one, with essentially no dependence on the quasienergy  $\epsilon_\alpha$ . For faster driving, however, the local particle number changes seemingly chaotically from one eigenstate to the next. The transition to the fast driving regime can also be appreciated from the range of quasi energies: outside the fast driving regime ( $\omega/J = 1$ ), the full interval  $[-\omega/2, \omega/2)$  is occupied, whereas the occupied interval hardly grows with increasing  $\omega$  for  $\omega/J \geq 4$ .

The width of the distribution of local particle numbers is best characterized in terms of the difference between the typical largest and typical smallest local particle number. Fig. 3b depicts the width  $\Delta \langle \hat{n}_{L/2} \rangle = \langle \hat{n}_{L/2} \rangle_{\text{max}} - \langle \hat{n}_{L/2} \rangle_{\text{min}}$ , where  $\langle \hat{n}_{L/2} \rangle_{\text{max/min}}$  is the average over the 20 largest/lowest local particle numbers. The error bars are estimated from the variances of these averages. The dependence of  $\Delta \langle \hat{n}_{L/2} \rangle$  on the driving frequency  $\omega$ , shows a well-pronounced increase indicating the formation of many-body scars on the transition to the high-frequency regime.

Having established the appearance of quantum many-body scars, the last – but crucial – aspects to discuss are their experimental signatures and realization.

*Coherent Oscillations.* – A direct way of detecting scarred states is by studying the long time oscillations of specially prepared initial states. For the optimal parameters in the high-frequency limit, the state will remain in the subspace of its fragment and thus show coherent oscillations. If the driving frequency is finite, but sufficiently large so that the rates of leaking channels are much smaller than tunnelings rates within the subspace,

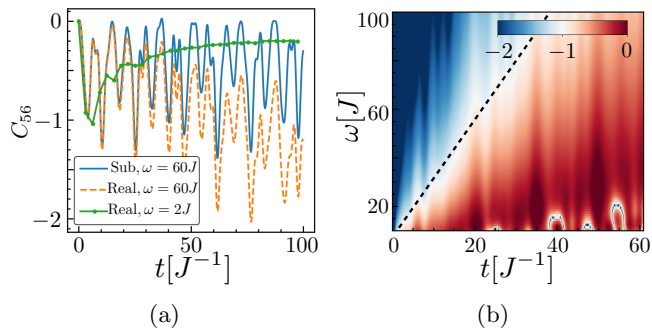


FIG. 4: (a) Correlation function given optimal parameters. Coherent oscillation with fast driving matches well with subsystem approximation, indicating the existence of scarred states. In contrast, correlation saturates quickly in the ergodic case with  $\omega = 2J$  where higher order effects induce deleterious leaking. (b)

Correlation difference  $\log_{10}(R(t))$  between real dynamics and subspace approximation (Eq. (10)) for varying frequencies. Some blue spots appear within the red region at longer times because of the accidental similarity between  $C_{\text{real}}(t)$  and  $C_{\text{sub}}(t)$ .

these coherent oscillations will be damped out slowly and their lifetime can exceed the thermalization time by far.

As a specific example, we focus on the stroboscopic dynamics of a system with ten sites with periodic boundary conditions and initialized in the Fock state  $|1100330011\rangle$ . The coherent oscillation of the two-point correlation function  $C_{56}(t) = \langle \hat{n}_5(t)\hat{n}_6(t) \rangle - \langle \hat{n}_5(t) \rangle \langle \hat{n}_6(t) \rangle$ , of the two central sites is depicted in Fig. 4a. The actual system dynamics  $C_{\text{real}}(t)$  are depicted in orange and compared to the dynamics  $C_{\text{sub}}(t)$  induced by the subsystem Hamiltonian [43] in which all rates of leaking channels are set to vanish. The ergodic case with slow driving is depicted in green, and it shows that the correlation saturates rapidly on a time-scale  $t \sim O(1/J)$ . While the comparison between actual scar dynamics and the effective subsystem dynamics gives evidence of damping due to leakage, the oscillations in the scarred dynamics also clearly exceed the time-scale of thermalization.

In order to turn this qualitative observation into a quantitative assessment of the lifetime of the coherent oscillations, it is helpful to define the difference between the two correlation functions

$$R(t) = |C_{\text{real}}(t) - C_{\text{sub}}(t)|, \quad (10)$$

comparing the actual dynamics and the effective subsystem dynamics. The difference  $R(t)$  is depicted in log10 scale in Fig. 4b as a function of time  $t$  and driving frequency  $\omega$ . As one can see, the difference is very small (blue) for short times, and there is a clear increase (red) for longer times. The point in time around which this transition occurs grows linearly with  $\omega$ , as indicated by a dashed black line. This allows us to define lifetimes for

scar states. The proportionality to  $\omega$  indicates that the scar states become increasingly stable as the fast driving regime is approached ( $\omega \rightarrow \infty$ ).

Similar long-lived coherent dynamics, *e.g.* Bloch oscillations (BO), also appear in a static tilted lattice without driving [44, 45]. However, there are several crucial differences between BO and scar dynamics that can be employed to distinguish them, *e.g.* initial state dependency and stability to additional interactions, see more details in the Supplementary Material.

*Experimental Realization.*— The doubly modulated Hubbard system in cold atomic gases and the required initial states can be constructed via existing experimental techniques. The driving can be achieved by periodically modulating external magnetic fields in the vicinity of Feshbach resonances [39, 46] and lattice shaking [47]. In practice, there will be an additional, typically harmonic trapping potential; since it commutes with the driving term in the Hamiltonian (Eq.(1)), it does not contribute to the kinetic constraints resulting in the scar states. The remaining challenge is thus to prepare fine tuned initial states. The easiest states to verify fragmentation and violation of ETH are the Mott insulator state and the density wave state with two particles on every second site. Both of them are eigenstates of the effective Hamiltonian, thus, they will be frozen in the presence of fast driving. For more interesting cases discussed above, one can first prepare Mott states with three bosons per site [48] and then apply the single-spin addressing scheme [49] to remove unwanted particles on selected sites to obtain for example  $|\dots 003300003300\dots\rangle$ . This state provides an example which shows coherent oscillations for an exceptionally long time before thermalization in the high-frequency limit.

*Conclusions & Outlook.*— Our concrete proposal enables the experimental realization of quantum many-body scars in a bosonic system, allowing the study of thermalization and lack thereof in systems substantially larger than those possible to study in any theoretical analysis. The Floquet engineering of kinetically constrained hopping discussed here can be achieved independently of system dimensionality and geometry, thus paving the way to substantially deepen our understanding of different thermalization paths in two- and three-dimensional systems with different lattice geometries (some of which can result in topological order [50]).

The suppression of leaking channels, as well as kinetically constrained hopping in general, is not only helpful for enabling experiments for quantum many-body scars, but it can potentially also be used to suppress processes like heating [51] that poses a serious limitation to quantum simulations based on driven atomic gases. Finally, the ability to open and close selected tunneling channels also opens up new pathways for state preparation like the accurate creation of a coherent superposition of different Fock states [52] as required *e.g.* for precision sensing.

*Acknowledgements.*— We acknowledge helpful discussions with Monika Aidelsburger, Pablo Sala and Ana Hudomal.

---

\* hongzheng.zhao17@imperial.ac.uk

- [1] Anatoli Polkovnikov, Krishnendu Sengupta, Alessandro Silva, and Mukund Vengalattore. Colloquium: Nonequilibrium dynamics of closed interacting quantum systems. *Reviews of Modern Physics*, 83(3):863, 2011.
- [2] Marcos Rigol, Vanja Dunjko, and Maxim Olshanii. Thermalization and its mechanism for generic isolated quantum systems. *Nature*, 452(7189):854, 2008.
- [3] Immanuel Bloch. Ultracold quantum gases in optical lattices. *Nature Physics*, 10 2005.
- [4] Maciej Lewenstein, Anna Sanpera, Veronica Ahufinger, Bogdan Damski, Aditi Sen(De), and Ujjwal Sen. Ultracold atomic gases in optical lattices: mimicking condensed matter physics and beyond. *Advances in Physics*, 56(2):243–379, 2007.
- [5] Hannes Bernien, Sylvain Schwartz, Alexander Keesling, Harry Levine, Ahmed Omran, Hannes Pichler, Soonwon Choi, Alexander S Zibrov, Manuel Endres, Markus Greiner, et al. Probing many-body dynamics on a 51-atom quantum simulator. *Nature*, 551(7682):579, 2017.
- [6] Jan Benhelm, Gerhard Kirchmair, Christian F Roos, and Rainer Blatt. Towards fault-tolerant quantum computing with trapped ions. *Nature Physics*, 4(6):463, 2008.
- [7] Rainer Blatt and Christian F Roos. Quantum simulations with trapped ions. *Nature Physics*, 8(4):277–284, 2012.
- [8] Stefan Trotzky, Yu-Ao Chen, Andreas Fleisch, Ian P McCulloch, Ulrich Schollwöck, Jens Eisert, and Immanuel Bloch. Probing the relaxation towards equilibrium in an isolated strongly correlated one-dimensional bose gas. *Nature Physics*, 8(4):325, 2012.
- [9] Jae-yoon Choi, Sebastian Hild, Johannes Zeiher, Peter Schauß, Antonio Rubio-Abadal, Tarik Yefsah, Vedika Khemani, David A Huse, Immanuel Bloch, and Christian Gross. Exploring the many-body localization transition in two dimensions. *Science*, 352(6293):1547–1552, 2016.
- [10] Pasquale Calabrese, Fabian HL Essler, and Maurizio Fagotti. Quantum quench in the transverse-field ising chain. *Physical review letters*, 106(22):227203, 2011.
- [11] Rahul Nandkishore and David A Huse. Many-body localization and thermalization in quantum statistical mechanics. *Annu. Rev. Condens. Matter Phys.*, 6(1):15–38, 2015.
- [12] Dmitry A. Abanin, Ehud Altman, Immanuel Bloch, and Maksym Serbyn. Colloquium: Many-body localization, thermalization, and entanglement. *Rev. Mod. Phys.*, 91:021001, May 2019.
- [13] Thomas Kohler, Sebastian Scherg, Xiao Li, Henrik P. Lüschen, Sankar Das Sarma, Immanuel Bloch, and Monika Aidelsburger. Observation of many-body localization in a one-dimensional system with a single-particle mobility edge. *Phys. Rev. Lett.*, 122:170403, May 2019.
- [14] Christopher J Turner, Alexios A Michailidis, Dmitry A Abanin, Maksym Serbyn, and Z Papić. Weak ergodicity breaking from quantum many-body scars. *Nature Physics*, 14(7):745, 2018.
- [15] Soonwon Choi, Christopher J Turner, Hannes Pichler, Wen Wei Ho, Alexios A Michailidis, Zlatko Papić, Maksym Serbyn, Mikhail D Lukin, and Dmitry A Abanin. Emergent su(2) dynamics and perfect quantum many-body scars. *Physical Review Letters*, 122(22):220603, 2019.
- [16] Vedika Khemani, Chris R Laumann, and Anushya Chandran. Signatures of integrability in the dynamics of rydberg-blockaded chains. *Physical Review B*, 99(16):161101, 2019.
- [17] Kieran Bull, Ivar Martin, and Z. Papić. Systematic construction of scarred many-body dynamics in 1d lattice models. *Phys. Rev. Lett.*, 123:030601, Jul 2019.
- [18] Cheng-Ju Lin and Olexei I. Motrunich. Exact quantum many-body scar states in the rydberg-blockaded atom chain. *Phys. Rev. Lett.*, 122:173401, Apr 2019.
- [19] Cheng-Ju Lin, Anushya Chandran, and Olexei I Motrunich. Slow thermalization of exact quantum many-body scar states under perturbations. *arXiv preprint arXiv:1910.07669*, 2019.
- [20] Wen Wei Ho, Soonwon Choi, Hannes Pichler, and Mikhail D Lukin. Periodic orbits, entanglement, and quantum many-body scars in constrained models: Matrix product state approach. *Physical review letters*, 122(4):040603, 2019.
- [21] Shriya Pai, Michael Pretko, and Rahul M Nandkishore. Robust quantum many-body scars in fracton systems. *arXiv preprint arXiv:1903.06173*, 2019.
- [22] Bhaskar Mukherjee, Sourav Nandy, Arnab Sen, and K Sengupta. Collapse and revival of quantum many-body scars via floquet engineering. *arXiv preprint arXiv:1907.08212*, 2019.
- [23] Michael Schecter and Thomas Iadecola. Weak ergodicity breaking and quantum many-body scars in spin-1 xy magnets. *arXiv preprint arXiv:1906.10131*, 2019.
- [24] AA Michailidis, CJ Turner, Z Papić, DA Abanin, and M Serbyn. Slow quantum thermalization and many-body revivals from mixed phase space. *arXiv preprint arXiv:1905.08564*, 2019.
- [25] Sho Sugiura, Tomotaka Kuwahara, and Keiji Saito. Many-body scar state intrinsic to periodically driven system: Rigorous results. *arXiv preprint arXiv:1911.06092*, 2019.
- [26] Asmi Haldar, Diptiman Sen, Roderich Moessner, and Arnab Das. Scars in strongly driven floquet matter: resonance vs emergent conservation laws. *arXiv preprint arXiv:1909.04064*, 2019.
- [27] Pablo Sala, Tibor Rakovszky, Ruben Verresen, Michael Knap, and Frank Pollmann. Ergodicity-breaking arising from hilbert space fragmentation in dipole-conserving hamiltonians. *arXiv preprint arXiv:1904.04266*, 2019.
- [28] Sanjay Moudgalya, Stephan Rachel, B. Andrei Bernevig, and Nicolas Regnault. Exact excited states of nonintegrable models. *Phys. Rev. B*, 98:235155, Dec 2018.
- [29] Sanjay Moudgalya, Nicolas Regnault, and B. Andrei Bernevig. Entanglement of exact excited states of affleck-kennedy-lieb-tasaki models: Exact results, many-body scars, and violation of the strong eigenstate thermalization hypothesis. *Phys. Rev. B*, 98:235156, Dec 2018.
- [30] Thomas Iadecola, Michael Schecter, and Shenglong Xu. Quantum many-body scars from magnon condensation. *Phys. Rev. B*, 100:184312, Nov 2019.
- [31] Thomas Iadecola and Michael Schecter. Quantum many-body scar states with emergent kinetic constraints and finite-entanglement revivals. *Phys. Rev. B*, 101:024306,

- Jan 2020.
- [32] Sanjay Moudgalya, B Andrei Bernevig, and Nicolas Regnault. Quantum many-body scars in a landau level on a thin torus. *arXiv preprint arXiv:1906.05292*, 2019.
- [33] Giuseppe De Tomasi, Daniel Hetterich, Pablo Sala, and Frank Pollmann. Dynamics of strongly interacting systems: From fock-space fragmentation to many-body localization. *arXiv preprint arXiv:1909.03073*, 2019.
- [34] Ana Hudomal, Ivana Vasić, Nicolas Regnault, and Zlatko Papić. Quantum scars of bosons with correlated hopping. *arXiv preprint arXiv:1910.09526*, 2019.
- [35] Marin Bukov, Luca D'Alessio, and Anatoli Polkovnikov. Universal high-frequency behavior of periodically driven systems: from dynamical stabilization to floquet engineering. *Advances in Physics*, 64(2):139–226, 2015.
- [36] André Eckardt, Christoph Weiss, and Martin Holthaus. Superfluid-insulator transition in a periodically driven optical lattice. *Phys. Rev. Lett.*, 95:260404, Dec 2005.
- [37] Sebastian Greschner, Luis Santos, and Dario Poletti. Exploring unconventional hubbard models with doubly modulated lattice gases. *Phys. Rev. Lett.*, 113:183002, Oct 2014.
- [38] Hongzheng Zhao, Johannes Knolle, and Florian Mintert. Engineered nearest-neighbor interactions with doubly modulated optical lattices. *Phys. Rev. A*, 100:053610, Nov 2019.
- [39] Cheng Chin, Rudolf Grimm, Paul Julienne, and Eite Tiesinga. Feshbach resonances in ultracold gases. *Rev. Mod. Phys.*, 82:1225–1286, Apr 2010.
- [40] Ph. Courteille, R. S. Freeland, D. J. Heinzen, F. A. van Abeelen, and B. J. Verhaar. Observation of a feshbach resonance in cold atom scattering. *Phys. Rev. Lett.*, 81:69–72, Jul 1998.
- [41] Andre Eckardt and Egidijus Anisimovas. High-frequency approximation for periodically driven quantum systems from a floquet-space perspective. *New Journal of Physics*, 17(9):093039, 2015.
- [42] Albert Verdeny and Florian Mintert. Tunable chern insulator with optimally shaken lattices. *Phys. Rev. A*, 92:063615, Dec 2015.
- [43] C. J. Turner, A. A. Michailidis, D. A. Abanin, M. Serbyn, and Z. Papić. Quantum scarred eigenstates in a berg atom chain: Entanglement, breakdown of thermalization, and stability to perturbations. *Phys. Rev. B*, 98:155134, Oct 2018.
- [44] Zachary A. Geiger, Kurt M. Fujiwara, Kevin Singh, Ruwan Senaratne, Shankari V. Rajagopal, Mikhail Lipatov, Toshihiko Shimasaki, Rodislav Driben, Vladimir V. Konotop, Torsten Meier, and David M. Weld. Observation and uses of position-space bloch oscillations in an ultracold gas. *Phys. Rev. Lett.*, 120:213201, May 2018.
- [45] Andreas Buchleitner and Andrey R Kolovsky. Interaction-induced decoherence of atomic bloch oscillations. *Physical review letters*, 91(25):253002, 2003.
- [46] F. Meinert, M. J. Mark, K. Lauber, A. J. Daley, and H.-C. Nägerl. Floquet engineering of correlated tunneling in the bose-hubbard model with ultracold atoms. *Phys. Rev. Lett.*, 116:205301, May 2016.
- [47] Pranjal Bordia, Henrik Lüschen, Ulrich Schneider, Michael Knap, and Immanuel Bloch. Periodically driving a many-body localized quantum system. *Nature Physics*, 13(5):460–464, 2017.
- [48] Jacob F. Sherson, Christof Weitenberg, Manuel Endres, Marc Cheneau, Immanuel Bloch, and Stefan Kuhr. Single-atom-resolved fluorescence imaging of an atomic mott insulator. *Nature*, 467(7311):68–72, 2010.
- [49] Christof Weitenberg, Manuel Endres, Jacob F. Sherson, Marc Cheneau, Peter Schauß, Takeshi Fukuhara, Immanuel Bloch, and Stefan Kuhr. Single-spin addressing in an atomic mott insulator. *Nature*, 471(7338):319–324, 2011.
- [50] Seulgi Ok, Kenny Choo, Christopher Mudry, Claudio Castelnovo, Claudio Chamon, and Titus Neupert. Topological many-body scar states in dimensions 1, 2, and 3. *arXiv preprint arXiv:1901.01260*, 2019.
- [51] Achilleas Lazarides, Arnab Das, and Roderich Moessner. Equilibrium states of generic quantum systems subject to periodic driving. *Phys. Rev. E*, 90:012110, Jul 2014.
- [52] Christie S. Chiu, Geoffrey Ji, Anton Mazurenko, Daniel Greif, and Markus Greiner. Quantum state engineering of a hubbard system with ultracold fermions. *Phys. Rev. Lett.*, 120:243201, Jun 2018.

### Comparison between Bloch Oscillations and Scar Dynamics

With tilted lattices, non-interacting atoms can show long-lived Bloch oscillation (BO) [44, 45]. However, there are several crucial differences between BO and the coherent scar dynamics (Fig. 4a) which can be employed to distinguish them experimentally.

First, in contrast to BO, the existence of the coherent oscillation presented in the main content strongly depends on the specially selected initial conditions. Only properly prepared initial states, *e.g.* Fock states constructed with building blocks, can exhibit coherent dynamics. Alternatively, the Mott and density wave states are dynamically frozen for fast driving. As a counterexample, the superfluid state will thermalize very quickly. Moreover, the oscillating frequency of BO is fixed by the tilted potential [44], while for the coherent scar dynamics, it can vary by choosing different initial states.

Second, in the presence of additional interactions (of energy scale  $U$  comparable to bare tunneling  $J$ ), BO are very sensitive to interaction-induced dephasing and instabilities thus decay rapidly [45]. Yet this is not true

for scar dynamics. Interactions commute with the unitary transformation to the rotating frame thus can be simply added to the lowest order effective Hamiltonian (Eq. 2) as it is. Therefore, the density assisted tunneling will not be impacted and the kinetic constraints leading to Hilbert space fragmentation remain unchanged. Considering higher-order processes, our previous work [38] showed that only negligible ( $1/\omega^2$ ) effects are induced, therefore the coherent oscillation will still persist for a long time with fast driving.

Third, the correlation between different building blocks serves as a good measure since no tunnelling is permitted in-between in the effective Hamiltonian. As an example, for the initial state  $|1100330011\rangle$ , the correlation function  $C_{15}(t) = \langle \hat{n}_1(t) \hat{n}_5(t) \rangle - \langle \hat{n}_1(t) \rangle \langle \hat{n}_5(t) \rangle$  remains zero for a sufficiently long time with fast driving. On the contrary, BO will build up such a spatial correlation after a short period.

All these three aspects exploit the many-body character of the density assisted tunneling which does not have a counterpart in non-interacting systems. Importantly, they are experimentally verifiable via local occupation number or two-point correlation functions.